Bioconjugated Re(I) complexes with amino acid derivatives: synthesis, photophysical properties and cell imaging studies

*Vanesa Fernández-Moreira,[a] Mª Lourdes Ortego,[a] Catrin F. Williams,[c] Michael P. Coogan,[b] Mª Dolores Villacampa[a] and Mª Concepción Gimeno[a]**

(a) ISQCH-Instituto de Síntesis Química y Catálisis Homogénea, Facultad de Ciencias, Universidad de Zaragoza-CSIC, C/ Pedro Cerbuna, 12, Zaragoza, 50009, Spain

(b) School of Chemistry, Cardiff University, Cardiff, Wales, UK CF10 3AT.

(c) School of Biosciences, Cardiff University, Cardiff, Wales, UK CF10 3AT

AUTHOR EMAIL ADDRESS: gimeno@unizar.es

ABSTRACT. The synthesis of a series of bioconjugated *fac* tricarbonyl rhenium bisimine complexes with amino acid ester derivatives and their application in fluorescent microscopy cell imaging is reported. A range of *meta* and *para*-bioconjugated pyridyl derivatives were synthesized and their photophysical properties were analyzed upon coordination to *fac*-[Re(bipy)$(CO)_3(CF_3SO_3)$]. Their long lifetimes (270 – 370 ns) and large Stokes shifts (>140 nm) suggested the new bioconjugated rhenium complexes as strong candidates for cell imaging applications. All species were taken up by MCF-7 cells and seemed to have a distinct localization pattern. However, while cells incubated with *para*-derivatives had an anomalous cellular growth pattern and suffered from photobleaching upon irradiation promoting cellular death, those incubated with the *meta*-derivatives behaved in a normal manner and did not photobleach, emphasizing the importance of the ligand design when it comes to have an optimum outcome, *i.e.* cell imaging or photo-therapy applications.

INTRODUCTION. Optimum detection of individual biomolecules, cell components and other biological entities, as well as targeting of drugs is becoming one of the most important issues in medicine. In order to respond to this demand, the use of luminescent visualization techniques is receiving great attention due to their non-invasive character, and consequently, there is a growing number of reports dealing with the application of phosphorescent d^6 metal complexes as luminophores in cell imaging.[1] In particular, derivatives of *fac*-{Re^{I}(bisimine)$(CO)_3$} core have attractive intrinsic photophysical properties such as large Stokes shift, long luminescent lifetimes, visible light excitation and emission, resistance to photobleaching among others, which make them excellent candidates for applications in cell imaging.[2] Large Stokes shifts (hundred of nm) will prevent self-quenching processes (re-absorption of emitted light) and will allow to

distinguish easily the emission of the fluorophores from the autofluorescence (emission from endogenous fluorophores, typically Stokes shift of tens of nm). In the same manner, long luminescent lifetime probes can be also used to filter out short–life autofluorescence via either time gating techniques or phase based techniques.[3] Visible light excitation and emission avoids problems of UV-tissue damage and low photobleaching character prevents formation of non-emissive products which is normally due to the reaction of exited state of a luminophore with oxygen. In addition to the advantageous photophysical properties of *fac*-{Re^{I}(bisimine)$(CO)_3$} core, they have often also showed good biocompatibility features, such as very little or no intrinsic toxicity, stability in physiological conditions, cell uptake and localization in different mammalians cell lines (usually human carcinoma cell lines, either HeLa or MCF-7) which can be controlled by polarity factors and/or reactivity of the ligands of the coordination sphere.[4] In this context, the introduction of biomolecules within the imaging agent seems to be an optimum approach to avoid disruption of the organism and to promote cell permeability and localization within a specific area. Conjugation of d^6 complexes to biomolecules such as estradiol, oligopeptides, peptides and proteins is becoming a common strategy to assist in cellular uptake or to allow the sensing of other biomolecules by luminescence modulation upon interaction between these species.[5] In addition, a great number of reports have been also published dealing with the conjugation of d^6 metal complexes to biotin, which apart from their relevance in uptake processes as biotinylated species can be actively transported into cell, also are attractive in many biotin-avidin assays.[6] In the particular case of bioconjugated Re(I) derivatives as cellular probes, some examples on peptide,[7] different vitamines[8] and biotin[9] conjugates have been reported. However, conjugation of simpler biomolecules such amino acid derivatives and the study of their effect in cellular uptake, localization pattern and toxicity has not, to the best of our knowledge, yet been performed. In many cases localization can be explained in terms of simple chemical

processes, *e.g.* ionic, hydrophobic, electrostatic hydrogen bonding interactions, however, in some others the picture is more complex. Incorporation of amino acid derivatives into the core structure of parent rhenium complexes should endow the novel bioconjugated species with a more friendly recognition process by mammalian cells and therefore have drastic effects in properties such as toxicity, localization, etc. Modulation of these features is an effective tool to successfully develop bioprobes suitable for different applications *i.e.* cell imaging or photodynamic therapy.[10] In that line, the study of luminescent *fac*-$\{Re^{I}(bipy)(CO)_3X\}^{+}$ species, where X represents a pyridyl conjugated with an amino acid derivative in *meta* and *para*-position, seems to be an optimum approach for obtaining information about the influence of such group into the behavior of these species *in vivo*. The criterion for the election of the pyridyl unit over the diimine to perform the amino acid conjugation is conditioned by photophysical factors. Structural modification of diimine unit could affect drastically to the emissive properties of this type of species, as the phosphorescence observed is generally due to ^{3}MLCT transitions, specifically a $d\pi(Re) \rightarrow \pi^*$(diimine) transition. Therefore, variation of the pyridyl unit instead of the diimine will provide a feasibility study of the biological activity whereas the luminescent properties are retained.

EXPERIMENTAL SECTION

General measurement and Analysis

Instrumentation. C, H, and N analysis were carried out with a PERKIN-ELMER 2400 microanalyzer. Mass spectra were recorded on a BRUKER ESQUIRE 3000 PLUS, with the electrospray (ESI) technique and on a BRUKER MICROFLEX (MALDI-TOF). ^{1}H, ^{13}C{H} and ^{19}F NMR, including 2D experiments, were recorded at room temperature on a BRUKER AVANCE 400 spectrometer (^{1}H, 400 MHz, ^{13}C, 100.6 MHz, ^{19}F, 376.5 MHz) with chemical shifts (δ, ppm) reported relative to the solvent peaks of the deuterated solvent.[19] Room temperature steady-state emision and excitation spectra were recorded with a Jobin-Yvon-Horiba fluorolog FL3-11 spectrometer fitted with a JY TBX picosecond detection module. Luminescence lifetimes decays were obtain using a nanosecond flash-lamp 5000F and the data analyzed with the provided software package DAS6. UV/vis spectra were recorded with a 1cm quartz cells on an Evolution 600 spectrophotometer.

Crystal Structure Determinations. Data were registered on a Bruker Smart 1000 CCD diffractometer. The crystals were mounted in inert oil on glass fibres and transferred to the cold gas stream of the diffractometer. Data were collected using monochromated MoKα radiation (λ = 0.71073) in ω-scans. Absorption corrections based on multiple scans were applied with the program SADABS. The structures were solved by direct methods and refined on F^2 using the program SHELXL-97.[11] All non-hydrogen atoms were refined anisotropically. Hydrogen atoms of **L2** were located in the diffraction map. Hydrogen atoms of complex **Re-2** were included using a riding model. Further crystal data are given in Table 2 MoKα measured Friedel data cannot be

used to determine absolute structure in a light- atom study as compound **L2**, but data of the complex **Re-2** showed unambiguously that the asymmetric carbon atoms, C20 and C50, retained, as expected, the S-configuration of the commercial valine-methyl ester used in the synthesis of **L2**.

Human Cell Incubation Studies

Human adenocarcinoma cells (MCF-7), obtained from the European Collection of Cell Cultures, Porton Down,Wiltshire, UK, were maintained in Hepes modified minimum essential medium (HMEM) supplemented with 10% fetal bovine serum, penicillin and streptomycin. Cells were detached from the plastic flask using trypsin-EDTA solution, and suspended in an excess volume of growth medium. The homogenous cell suspension was then distributed into 1 ml aliquots with each aliquot being subject to incubation with a different lumophore, final concentration 100 mg ml^{-1}, at 4ºC for 30 min. Cells were finally washed three times in phosphate buffer saline (PBS, pH 7.2), harvested by centrifugation (5 min, 800 g) and mounted on a slide for imaging. Preparations were viewed using a Leica TCS SP2 AOBS confocal laser microscope using x 63 or x 100 objective, with excitation at 405 nm and detection at 520-570 nm.

Materials and Procedures

Fac-[Re(bipy)$(CO)_3(CF_3SO_3)$] was prepared according to literature procedures.[12] **Re-3** and **Re-6**, specifically *fac*-[Re(bipy)$(CO)_3$(L-phenylalanine-N-(4-pyridylcarbonyl)-methyl ester)](CF_3SO_3), and *fac*-[Re(bipy)$(CO)_3$(L-phenylalanine-N-(3-pyridylcarbonyl)-methyl ester)](CF_3SO_3) have been prepared using a modified method to that one reported in the literature for the synthesis of the analogous hexafluorophospate salts,[13] see bellow. All other starting materials and solvents were purchased from commercial suppliers and used as received unless otherwise stated.

Generic synthesis of L(1-3). Isonicotinic acid chloride (4.08 gr, 20 mmol), triethylamine (3.42 ml, 22 mmol) and the correspondent L-amino acid methyl ester (20 mmol) were stirred in dry

DCM for 24h at room temperature under an argon atmosphere. Then an aqueous solution of $NaHCO_3$ was added to mixture and an extraction was performed (3 × 20 ml DCM). The combined organic layers were dried over $MgSO_4$ and filtered over celite. The volume was reduced until 10 ml and addition of hexane and/or diethylether afforded **L1-L3.**

L-alanine-N-(4-pyridylcarbonyl)-methyl ester, L1, white solid, 3.70 g, 89 % yield. ^{1}H NMR (Acetone-d_6) δ: 8.72 (m, 2H, *H*(2)), 8.22 (s br, 1H, *NH*), 7.78 (m, 2H, *H*(3)), 4.66 (qd, *J* = 7.3, 7.3 Hz, 1H, NHC*H*), 3.70 (s, 3H, COO*CH*$_3$), 1.48 (d, *J* = 7.3 Hz, 3H, CH*CH*$_3$). ^{13}C NMR (Acetone-d_6) δ: 174.4 (s, 1C, *C*OOCH$_3$), 166.6 (*C*ONH), 152.1 (2C, *C*(2)), 142.8 (*C*(4)), 122.9 (2C, *C*(3)), 53.2 (NH*CH*), 50.3 (COO*C*H$_3$), 18.3 (CH*C*H$_3$). IR (solid, cm^{-1}): 3296 (ν(NH)), 1731 ν(CO$_{carboxylate}$), 1645 ν(CO$_{amide}$), 1537 ν$_{sim}$(C=N). Elemental analysis for $C_{10}H_{12}N_2O_3$ requires C, 57.68; H, 5.81; N, 6.21; S, 13.45 %; found C, 57.42; H, 5.92; N, 6.34; S, 13,46 %.

L-valine-N-(4-pyridylcarbonyl)-methyl ester, L2, white solid, 4.30 g, 91 % yield, ^{1}H NMR (Acetone-d_6) δ: 8.71 (m, 2H, *H*(2)), 8.05 (s br, 1H, *NH*), 7.78 (m, 2H, *H*(3)), 4.57 (m, 1H, NHC*H*), 3.72 (s, 3H, COOC*H*$_3$), 2.26 (m, 1H, C*H*-(CH$_3$)$_2$), 1.01 (2d, *J* = 6.9 Hz, 6H, CH-(C*H*$_3$)$_2$). ^{13}C NMR (Acetone-d_6) δ: 173.6 (*C*OOCH$_3$), 167.4 (*C*ONH), 152.1 (2C, *C*(2)), 143.2 (*C*(4)), 123.2 (2C, *C*(3)), 60.2 (NH*C*H), 53.2 (COO*C*H$_3$), 32.4 (*C*H-(CH$_3$)$_2$), 20.4 (CH-(*C*H$_3$)$_2$), 19.8 (CH-(*C*H$_3$)$_2$). IR (solid, cm^{-1}): 3245 (ν(NH)), 1729 (ν(CO$_{carboxylate}$)), 1660 (ν(CO$_{amide}$)). Elemental analysis for $C_{12}H_{16}N_2O_3$ required C, 61.00; H, 6.83; N, 11.86 %, found C, 61.12; H, 6.84; N, 11.95 %.

L-phenylalanine-N-(4-pyridylcarbonyl)-methyl ester, L3, brown oil, 5.42 g, 95 % yield [13]

Generic synthesis of L(4-6). These species were prepared similarly to **L(1-3)** using nicotinic acid chloride instead of isonicotinic acid chloride.

L-alanine-N-(3-pyridylcarbonyl)-methyl ester, L4, white solid, 290 mg, 69 % yield. ^{1}H NMR (Acetone-d_6) δ: 9.08 (m, 1H, *H*(2)), 8.71 (m, 1H, *H*(6)), 8.23 (m, 2H, *H*(4)), 8.14 (s br, 1H, *NH*),

7.48 (m, 1H, *H*(5)), 4.66 (qd, *J*= 7.3, 7.3 Hz, 1H, NHC*H*), 3.70 (s, 3H, COOCH_3), 1.48 (d, *J* = 7.32 Hz, 3H, CHCH_3). ^{13}C NMR (Acetone-d_6) δ: 174.7 (*C*OOCH$_3$), 166.8 (*C*ONH), 1534.0 (2C, *C*(2)), 150.4 (2C, *C*(6)), 136.6 (*C*(4)), 131.6 (*C*(3)*)*, 125.1 (2C, *C*(5)*)*, 53.3 (NH*C*H), 50.3 (COO*C*H$_3$), 18.5 (CH*C*H$_3$). IR (solid, cm^{-1}): 3324 (ν(NH)), 1740 (ν(CO$_{carboxylate}$)), 1636 (ν(CO$_{amide}$)), 1524 ((ν(C=N)).

L-valine-N-(3-pyridylcarbonyl)-methyl ester, L5, white solid, 470 mg, 82 % yield. ^{1}H NMR (Acetone-d_6) δ: 9.07 (m, 1H, *H*(2)), 8.70 (m, 1H, *H*(6)), 8.23 (m, 2H, *H*(4)), 7.95 (s br, 1H, N*H*), 7.47 (m, 1H, *H*(5)), 4.58 (dd, *J* = 8.4, 6.4 Hz, 1H, NHC*H*), 3.72 (s, 3H, COOCH_3), 2.26 (m, 1H, C*H*-(CH$_3$)$_2$), 1.02 (dd, *J* = 8.7, 6.8 Hz, 6H, CH-(CH_3)$_2$). ^{13}C NMR (Acetone-d_6) δ: 173.8 (*C*OOCH$_3$), 167.5 (*C*ONH), 154.0 (2C, *C*(2)), 150.6 (2C, *C*(6)), 136.8 (*C*(4)), 131.9 (s, 2C, *C*(3)), 125.1 (s, 2C, *C*(5)), 60.1 (NH*C*H), 53.1 (COO*C*H$_3$), 32.4 (*C*H-(CH$_3$)$_2$), 20.5 (2C, CH-(*C*H$_3$)$_2$), 19.8 (2C, CH-(*C*H$_3$)$_2$). IR (solid, cm^{-1}): 3332 (ν(NH)), 1733 (ν(CO$_{carboxylate}$)), 1638 (ν(CO$_{amide}$)), 1522 ((ν(C=N)).

L-phenylalanine-N-(3-pyridylcarbonyl)-methyl ester, L6, light brown oil, 370 mg, 66 % yield.[13]

Synthesis of Re-1. [Re(bipy)(CO)$_3$(CF$_3$SO$_3$)] (205 mg, 0.36 mmol) and L-alanine-N-(4-pyridylcarbonyl)-methyl ester, **L1**, (223 mg, 1.07 mmol) were stirred in dry DCM (20 ml) for 12 h at room temperature under a nitrogen atmosphere. Then, the solvent was removed under vacuum and the product was purified by an alumina chromatographic column, starting from a mixture of solvents DCM:MeOH, (70:1) and increasing the polarity until (70:5). The second yellow fraction eluted was collected, evaporated and dried under vacuum to give complex **Re-1** as a yellow solid (75 mg, 27 %). ^{1}H NMR (Acetone-d_6) δ 9.49 (d, *J* = 5.4 Hz, 2H, C*H*(6) bipy), 8.80 – 8.65 (m, 4H, C*H*(3) bipy, C*H*(2) Py), 8.47 (t, *J* = 7.9 Hz, 2H, C*H*(4) bipy), 8.39 (s br, 1H, N*H*), 8.05 – 7.98 (m, 2H, C*H*(5) bipy), 7.81 (dd, *J* = 5.2, 1.5 Hz, 2H, C*H*(3) Py), 4.58 – 4.49 (m,

1H, C*H*(7)), 3.64 (s, 3H, OC*H*$_3$), 1.41 (d, *J* = 7.3 Hz, 3H, C*H*$_3$).^{13}C NMR (Acetone-d$_6$) δ 196.3 (*C*O), 192.5 (*C*O), 173.1 (*C*OO), 163.9 (*C*ON), 156.9 (*C*(2) bipy), 155.0 (*C*(6) bipy), 153.9 (*C*(2) py), 145.0 (*C*(4) py), 142.4 (*C*(4) bipy), 130.0 (*C*(5) bipy), 125.9 (*C*(3) bipy), 125.4 (*C*(3) py), 52.4 (*C*H), 49.7 (O*C*H$_3$), 17.2 (*C*H$_3$). IR (solid, cm^{-1}): 2029 (s, ν(CO)), 1905 ((m, ν(CO)). Elemental analysis for ReC$_{24}$H$_{20}$N$_4$O$_9$SF$_3$ requires C, 36.78; H, 2.57; N, 7.15 %; found C, 37.36; H, 2.78; N, 6.74 % . MS ES *m/z*: calculated for C$_{23}$H$_{20}$N$_4$O$_6$Re$^+$ (M$^+$) 634.6, found 634.8.

Synthesis of Re-2. This compound was prepared similarly to **Re-1** using L-valine-N-(4-pyridylcarbonyl)-methyl ester, **L2**, instead of L-alanine-N-(4-pyridylcarbonyl)-methyl ester, **L1**. The pure product was obtained as yellow solid (30% yield). ^{1}H NMR (Acetone-d$_6$) δ 9.49 (d, *J* = 5.5 Hz, 2H, *H*(6) bipy), 8.79 – 8.67 (m, 4H, C*H*(3) bipy, C*H*(2) Py), 8.48 (ddd, *J* = 8.1, 2.9, 1.5 Hz, 2H, C*H*(4) bipy), 8.11 (s br, 1H, N*H*), 8.06 – 7.97 (m, 2H, C*H*(5) bipy), 7.80 (dd, *J* = 5.2, 1.5 Hz, 2H, C*H*(3) Py), 4.51 – 4.42 (m, 1H, C*H*(7)), 3.67 (s, 3H, OC*H*$_3$), 2.19 (dq, *J* = 20.2, 6.7 Hz, 2H, C*H*(8)), 0.94 (dd, *J* = 6.8, 2.9 Hz, 6H, 2C*H*$_3$). ^{13}C NMR (Acetone-d$_6$) δ 197.30 (*C*O), 193.5 (*C*O), 172.2 (*C*OO), 164.7 (*C*ON), 156.9 (*C*(2) bipy), 155.0 (*C*(6) bipy), 153.8 (*C*(2) py), 145.2 (*C*(4) py), 142.4 (*C*(4) bipy), 130.1 (*C*(5) bipy), 125.9 (*C*(3) bipy), 125.5 (*C*(3) py), 59.4 (*C*H), 52.3 (O*C*H$_3$), 31.3 (*C*H$_2$), 19.4 (*C*H$_3$), 18.7 (*C*H$_3$). IR (solid, cm^{-1}): 2029 (s, ν(CO)), 1904 ((m, ν(CO)). Elemental analysis for ReC$_{26}$H$_{24}$N$_4$O$_9$SF$_3$ requires C, 38.42; H, 2.95; N, 6.89 %; found C, 38.83; H, 3.32; N, 7.47 %. MS ES *m/z*: calculated for C$_{25}$H$_{24}$N$_4$O$_6$Re$^+$ (M$^+$) 663.1, found 662.9.

Synthesis of Re-3. This compound was prepared similarly to **Re-1** using L-phenylalanine-N-(4-pyridylcarbonyl)-methyl ester, **L3**, instead of L-alanine-N-(4-pyridylcarbonyl)-methyl ester, **L1**. The pure product was obtained as yellow solid (20% yield). [13]

Synthesis of Re-4. The compound was prepared similarly to **Re-1** using L-alanine-N-(3-pyridylcarbonyl)-methyl ester, **L4**, instead of L-alanine-N-(4-pyridylcarbonyl)-methyl ester, **L1**.

The pure product was obtained as yellow solid (272 mg, 70% yield). ^{1}H NMR (Acetone-d_6) δ 9.50 (d, *J* = 5,4 Hz, 2H, C*H*(6) bipy), 8.87 – 8.80 (m, 1H, C*H*(2) py), 8.77 (d, *J* = 8.2 Hz, 2H, C*H*(3) bipy), 8.71 (dd, *J* = 5.7, 0.7 Hz, 1H C*H*(6) py), 8.65 – 8.52 (m, 2H, N*H*, C*H*(4) py), 8.51 – 8.41 (m, 2H, C*H*(4) bipy), 7.99-8.04 (m, 2H, C*H*(5) bipy), 7.56 (ddd, *J* = 8.0, 5.7, 0.6 Hz, 1H, C*H*(5) py), 4.51 (p, *J* = 7.3 Hz, 1H, C*H*(9)), 3.66 (s, 3H, OCH_3), 1.41 (d, *J* = 7.3 Hz, 3H, CH_3). ^{13}C NMR (Acetone-d_6) δ 196.3 (*C*O), 192.4 (*C*O), 173.2 (*C*OO), 163.3 (*C*ON), 156.8 (*C*(2) bipy), 155.1 (*C*(2) py), 154.9 (*C*(6) bipy), 152.4 (*C*(6) py), 142.4 (*C*(4) bipy), 139.2 (*C*(4) py), 133.2 (*C*(3) py), 130.0 (*C*(5) bipy), 127.4 (*C*(5) py), 126.0 (*C*(3) bipy), 52.4 (*C*H), 49.6 (O*C*H_3), 17.2 (*C*H_3). IR (solid, cm^{-1}): 2029 (s, ν(CO)), 1902 ((m, ν(CO)). Elemental analysis for $ReC_{24}H_{20}N_4O_9SF_3$ requires C, 36.78; H, 2.57; N, 7.15 %; found C, 37.43; H, 2.63; N, 7.34 %. MS ES *m/z*: calculated for $C_{23}H_{20}N_4O_6Re^+$ (M^+) 634.6, found 634.8.

Synthesis of Re-5. This compound was prepared similarly to **Re-1** using L-valine-N-(3-pyridylcarbonyl)-methyl ester, **L5**, instead of L-alanine-N-(4-pyridylcarbonyl)-methyl ester, **L1**. The pure product was obtained as yellow solid (134 mg, 70% yield). ^{1}H NMR (Acetone-d_6) δ 9.50 (d *J* = 5.4 Hz, 2H, C*H*(6) bipy), 8.84 – 8.74 (m, 4H, C*H*(3) bipy, C*H*(2,6) py), 8.54 – 8.44 (m, 3H, C*H*(4) bipy, C*H*(4) py), 8.00-8.07 (m, 3H, C*H*(5) bipy, N*H*), 7.60 (ddd, *J* = 8.0, 5.8, 0.5 Hz, 1H, C*H*(5) py), 4.44 (dd, *J* = 8.3, 6.4 Hz, 1H, C*H*(9)), 3.71 (s, 3H, OCH_3), 2.19 (dq, *J* = 13.5, 6.8 Hz, 1H, C*H*(10)), 0.95 (dd, *J* = 6.8, 5.1 Hz, 6H , 2CH_3). ^{13}C NMR (Acetone-d_6) δ 196.3 (*C*O), 192.3 (*C*O), 172.3 (*C*OO), 164.2 (*C*ON), 156.9 (*C*(2) bipy), 155.3 (*C*(2) py), 154.9 (*C*(6) bipy), 152.2 (*C*(6) py), 142.5 (*C*(4) bipy), 139.3 (*C*(4) py), 133.6 (*C*(3) py), 130.1 (*C*(5) bipy), 127.5 (*C*(5) py), 126.0 (*C*(3) bipy), 59.4 (*C*HN), 52.3 (O*C*H_3), 31.2 (*C*H), 19.4 (*C*H_3), 18.8 (*C*H_3). Elemental analysis for $ReC_{26}H_{24}N_4O_9SF_3$ requires C, 38.42; H, 2.95; N, 6.89 %; found C, 38.76; H, 3.11; N, 7.08 % IR (solid, cm^{-1}): 2029 (s, ν(CO)), 1904 ((m, ν(CO)). found C 38.83; H, 3.32; N 7.47 %. MS ES *m/z*: calculated for $C_{25}H_{24}N_4O_6Re^+$ (M^+) 663.1, found 662.8.

Synthesis of Re-6. This compound was prepared similarly to **ReL1** using L-phenylalanine-N-(3-pyridylcarbonyl)-methyl ester, **L6**, instead of L-alanine-N-(4-pyridylcarbonyl)-methyl ester, **L1**. The pure product was obtained as yellow solid (330 mg, 90% yield). [13]

RESULTS AND DICUSSION

Synthesis of ligands and complexes

Pyridyl-amino acid derivatives (**L1-6**) were synthesized by reaction of either, commercially available isonicotinic acid chloride or nicotinic acid chloride with the corresponding amino acid methyl ester derivative in presence of triethylamine to assist the condensation reaction (Scheme 1). Infrared spectroscopy showed the displacement of the $\upsilon(CO_{acyl})$ band from *ca.*1750 cm^{-1} to a $\upsilon(CO_{amide})$ at *ca.* 1650 cm^{-1} indicating the successful condensation reaction. Synthesis of the cationic rhenium derivatives, **Re(1-6)** see Table 1, was achieved by following literature precedents.[4] This involved initial formation of rhenium tricarbonyl bipyridyl chloride, then activation of the chloride by exchange to triflate to allow its final displacement for the desired pyridyl derivative (**L1-6**) under mild conditions, Scheme 2. Spectroscopy characterization of each ligand and rhenium complex was performed using IR, ^{1}H, ^{13}C-NMR, and UV-vis. Infrared spectra of rhenium complexes **Re(1-6)** showed two bands corresponding to the $\upsilon(CO)$ symmetric and asymmetric stretching modes at *ca.* 2029 (s) and 1904 (br) cm^{-1} respectively, which are typical of these type of cationic species with a C_{3v} symmetry. The higher energy band arises from an A_1 mode whereas the lower energy band, a broad band, is due to an E mode.[14] Moreover, ^{1}H-NMR spectra in acetone-d_6 showed, in all cases, a characteristic low field shift of the bipyridine protons *H*(6), from 9.0 to 9.5 ppm, indicative of the successful displacement of the triflate ligand for the pyridine derivatives (**L1-6**). Further analytical data for each complex was provided through elemental analysis and mass spectroscopy, which corroborate the accomplishment on the

synthesis of the bioconjugated rhenium(I) species **Re(1-6)**. Additionally, crystals of **Re-2** and **L2** suitable for X-ray analysis (SHELX programs) were obtained by slow evaporation of a CH_3OH solution and slow diffusion of a mixture of acetone-hexane solution, respectively.

Table 1. Numbered scheme for the synthesized rhenium species.

AA-derivatives	Ala	Val	Phe
para-Re species	**Re-1**	**Re-2**	**Re-3**
meta-Re species	**Re-4**	**Re-5**	**Re-6**

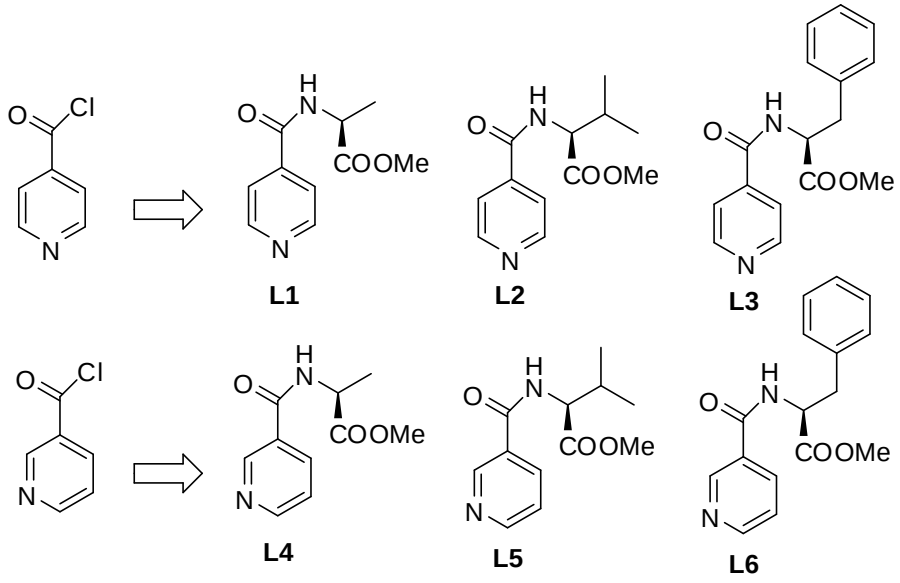

Scheme 1. Depiction of selected ligands and their precursors.

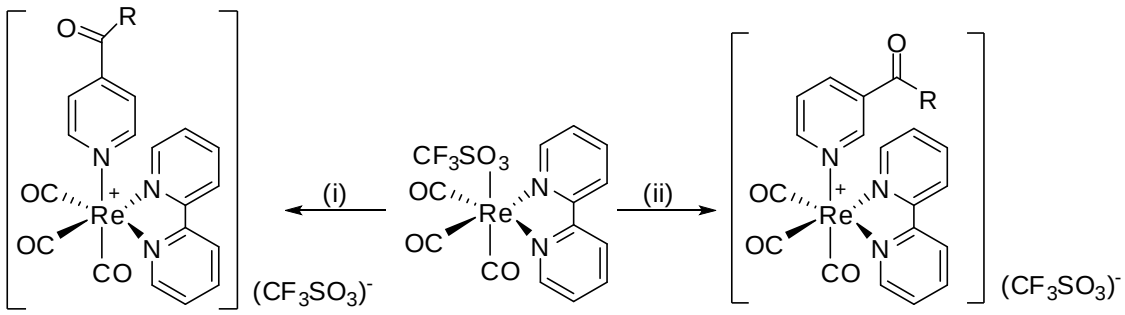

Re(1-3) **Re(4-6)**

R: L-alanine methyl ester (**Re-1**, **Re-4**)
L-valine methyl ester (**Re-2**, **Re-5**)
L-phenyl alanine methyl ester (**Re-3**, **Re-6**)

Scheme 2. Synthesis of rhenium complexes **Re(1-6)** ((i**) L(1-3)**, DCM, rt, 12h, argon atmosphere, (ii) **L(4-6)**, DCM, rt, 12h, argon atmosphere.

Luminescence properties of complexes

The electronic spectra of species **Re(1-6)** were recorded in DCM solution and showed the typical characteristic associated with bisimine Re(I) derivatives, *i.e.* two common features, ligand centered transitions (bipyridine, pyridine) at higher energy (< 320 nm) and metal-to-ligand-charge-transfer transitions (^{1}MLCT) at lower energy (345-360 nm). Specifically, **Re(4-6)** complexes, derived from the *meta*-substituted ligands have a slightly red shifted ^{1}MLCT transition compared to the *para*-analogues, see Figure 1, indicating that the main orbitals implicated in the transition are those belonging to the Re(dπ) and bipy(π*), whereas some contribution from the pyridine based orbitals is assumed in **Re(1-3)**. Relevant spectroscopic data are listed in Table 2. Direct irradiation of the ^{1}MLCT bands using excitation wavelengths between 350 and 410 nm gave a structureless visible emission centered at *ca.* 537 nm in the case of complexes **Re(1-3)** and at *ca.* 540 nm for **Re(4-6)** and thus, once again, a small red shift was observed on going from *para*-rhenium derivatives to *meta*-rhenium derivatives, Figure 2. Such

features are typical of cationic bisimine Re(I) complexes where the emission is frequently assigned as long-lived ^{3}MLCT in origin, specifically dπ(Re) $\rightarrow$ π^*(bipy). Luminescent lifetime measurements of each complex performed in degassed DCM showed a good fitting to a single exponential (indicative of one excited state environment) in the 267-374 ns domain, consistent with phosphorescent emission from a ^{3}MLCT state for complexes of the type *fac*-[Rebipy(CO)$_3$(L)]$^+$.[15] The longer lifetimes observed in DCM in comparison with those reported in the literature for similar complexes in CH_3CN, $\tau \approx 100 - 200$ ns, can be rationalized in terms of the greater stabilization of MLCT excited state in polar solvents, *i.e.* lowering the MLCT excited state energy allows non-radiative processes to occur easily.[16] Further lifetime data were recorded in CH_3CN solution for species **Re-2**, **Re-4** and **Re-5**. Lifetime values are in the range of 140 – 150 ns which corroborate the hypothesis of a greater MLCT excited state stabilization, see Table 1. As expected, maxima emission wavelength in CH_3CN solution were also shifted from *ca.* 539 to *ca.* 553 nm in concordance with the greater stabilization of the excited state in polar solvents.

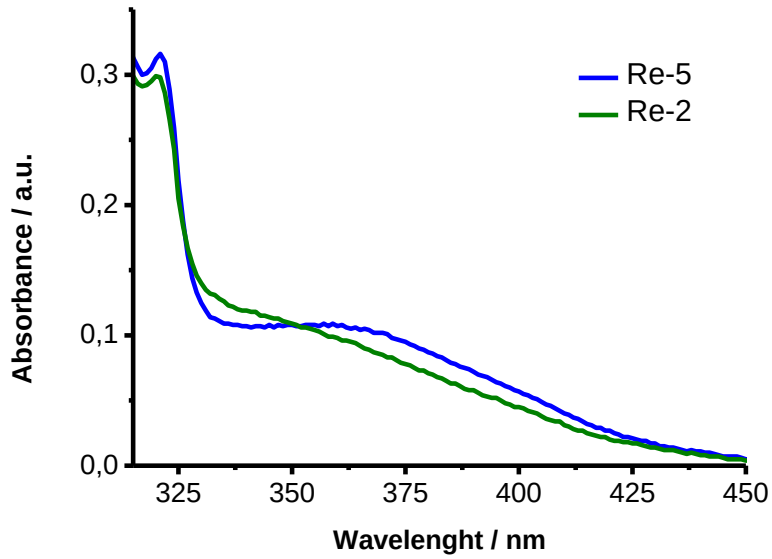

Figure 1. UV-absorption spectra for complexes **Re-2** and **Re-5** in DCM at 298K.

Table 2. Photophysical data of complexes **Re(1-6)** in degassed solutions of DCM and CH_3CN at 298K.

Complex	λ_{exc}/nm	λ_{em}/nm	T_{3MLCT}/ns[a]	λ_{abs} (^{1}MLCT)/nm (ε/dm^{3}mol^{-1}cm^{-1})
Re-1	401	537	320	351 (4200)
Re-2	366	538	374	352 (6720)
		553[b]	151[b]	
Re-3	358	537	327	348 (4320)
Re-4	371	540	267	355 (4280)
		554[b]	146[b]	
Re-5	417	541	374	359 (4360)
		553[b]	140[b]	
Re-6	410	540	370	359 (3960)

a) degassed DCM solution, b) degassed CH_3CN solution

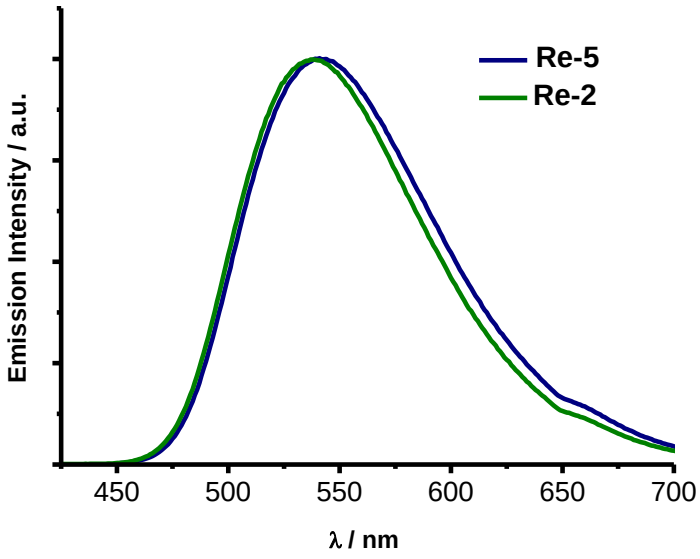

Figure 2. Emission spectra for complexes **Re-2** and **Re-5** in degassed DCM at 298K.

X-Ray Crystallography.

Ligand **L2** crystallized in space group $P2_12_12_1$ with a single molecule per asymmetric unit, Figure 3. Selected bond distances and angles are collected in Table 3. Structural parameters showed normal values. Additionally, **L2** displayed an intermolecular, short and reasonably linear H-bond [H6⋯N1# (#: -x+2, y-1/2, -z+1/2) 2.24(2) Å; N2-H6⋯N1 168.6(16)º] between the N-H amide group and the pyridinic N atom of one adjacent molecule. Such strong interaction led to an infinite chain of molecules (see Figure S1 in supporting information).

Complex **Re-2** crystallized in space group P2(1)/c with two rhenium complexes per asymmetric unit, see Table S1 in supporting information; these two molecules differ slightly in angles and bond distances. The coordination sphere of each rhenium unit can be described as a slightly distorted octahedron in which the three carbonyl ligands are arranged in a facial geometry, Figure 4. In both cases, the equatorial plane is described by the chelate bipyridine ligand and two *trans*-carbonyls. A third carbonyl and the pyridine derivative are placed in the apical plane. Deviation from the ideal octahedron is mostly originated from the geometric restraints imposed by the chelated ligand, with a chelate angle of N(1)Re(1)N(2): 75.70(4)º and N(5)Re(2)N(6):75.65(7)º instead of the ideal 90, and a slight deviation from planarity (torsion angle N(1)C(5)C(6)N(2): 2.7(2)º and N(5)C(35)C(36)N(6): 2.4(3)º as a result of packaging forces). Both of them showed a pair of mutual N-H⋯O close contacts [H4A⋯ O12# (# : x, y-1, z) 2.228 Å, N4-H4A⋯ O12 155.14º and H8A⋯O6# (# : x, y+1, z) 2.042 Å, N8-H8A⋯O6 169.99º] between the NH of one complex and the oxygen of the carbonyl methyl ester derivative of an adjacent molecule indicative of mutual hydrogen bonding, Figure 5. As expected, the asymmetric carbon atoms, C25 and C50, retained the S-configuration of the commercial valine-methyl ester used in the synthesis of **L2**. In addition, bond length and angles were within the expected range for analogous complexes reported in the literature, see legend in Figure 4**.**[4,17]

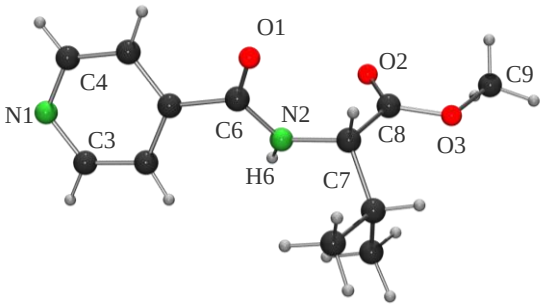

Figure 3. Ortep representation of complex **L2**.

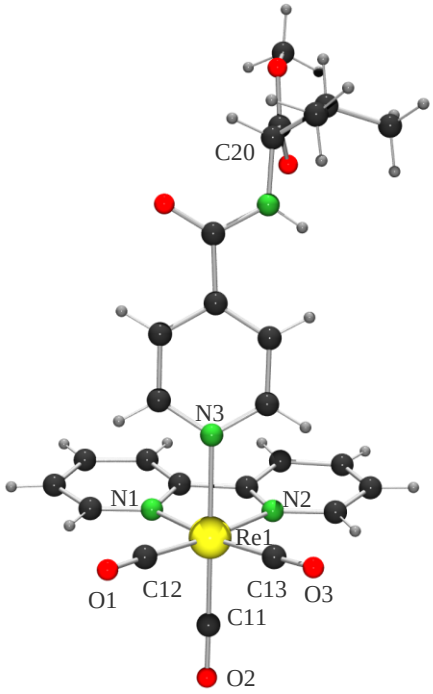

Figure 4. Ortep representation of complex **Re-2** (the second molecule within the asymmetric unit and the counter ions were omitted for clarity). The most relevant geometric parameters are: Re(1)-C(11): 1.912(14) Å, Re(1)-C(13): 1.924(15) Å, Re(1)-C(12): 1.933(11) Å, Re(1)-N(1): 2.127(12) Å, Re(1)-N(2): 2.156(10) Å, Re(1)-N(3): 2.187(9) Å, N(1)-Re(1)-N(2): 75.7(4)º, C(11)-Re(1)-N(3): 175.3(4)º, C(11)-Re(1)-C(13): 88.9(5)º, C(11)-Re(1)-C(12): 87.4(5)º, C(12)-Re(1)-N(1): 99.3(4)º, C(11)-Re(1)-N(2): 95.4(5)º.

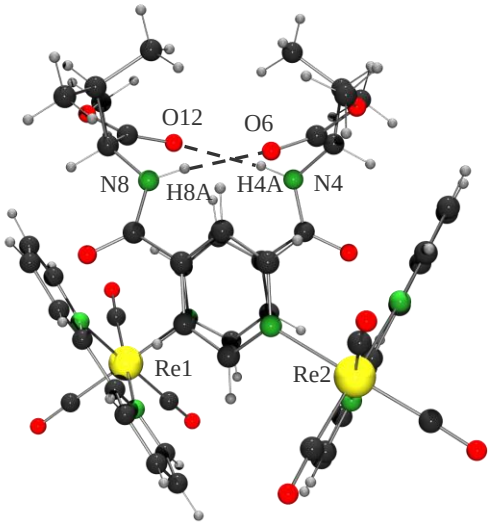

Figure 5. Ortep representation of adjacent molecules of complex **Re-2** showing the interaction N-O (--).

Table 3. Selected bond lengths [Å] and angles [°] for **L2**.

C(1)-C(6)	1.508(2)	C(6)-N(2)	1.345(2)
C(6)-O(1)	1.2263(18)	N(2)-C(7)	1.452(2)
O(1)-C(6)-N(2)	123.88(14)	N(2)-C(6)-C(1)	115.88(13)
O(1)-C(6)-C(1)	120.23(14)	C(6)-N(2)-C(7)	121.09(13)

Cellular studies and confocal microscopy

Having established that complexes **Re(1-6)** possessed the required photophysical properties for application in fluorescent cell imaging, a series of experiments were undertaken in which they were incubated with MCF-7 (human adenocarcenoma) cells. Incubation was performed at 4^{o} C to suppress active transport uptake mechanisms and to prevent encapsulation in endosomes. Following incubation and washing to remove agent from the medium, the cells were allowed to attain ambient temperature to grant biological processes to reactivate, and permitting cellular distribution mechanisms to operate. The results of the cell imaging experiments demonstrate that small changes in ligand structure can have a vital role in the biological properties of imaging agents. While the analogous pairs of agents from the series of complexes **Re(1-3)** and **Re(4-6)** bear identical substituents, and thus have similar solubilities, lipophilicities, etc; their behaviour in the cell experiments was markedly different. Whereas the pairs of complexes each showed good uptake, the effect on the cells was dramatically different: *para* substituted analogues **Re(1-3)** had a dramatic effect on the cells, with cell structure being badly damaged and clustering of dead and dying cells being observed in all cases, see Figure 7 (A-C). Although, a small number of cells showed healthy structures and the typical pattern of localisation of monocationic Re complexes with some general cytoplasmic staining and more intense mitochondrial localisation, see Figure 7 (D), the bulk of the populations were damaged and clustered indicating that these complexes have limited use as imaging agents.

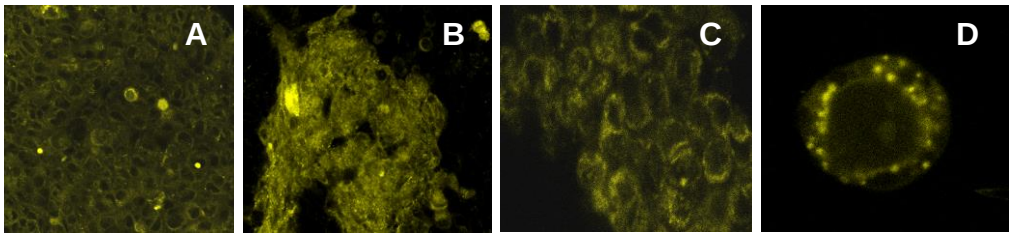

Figure 7. Cell imaging with complex **Re-1, Re-2** and **Re-3** showing clustering (picture A, B and C respectively) and cell imaging with complex **Re-2** showing localisation (picture D).

In addition, these samples showed considerable photobleaching, with z-stacking being impossible due to the loss of image intensity upon irradiation. Interestingly, the only previous report of significant damage to cell morphology across an entire cell sample and associated photobleaching was in the first published article dealing with the application of rhenium bipyridines in cell imaging, and was restricted to the case of a chloride complex.[18] In this case both, the toxicity and photobleaching, were assigned to lability of the halide, allowing interaction with biological donors, and subsequent photoreactivity upon irradiation. While there are many reports of variations in cytotoxicity of rhenium tricabonyl bipyridine-pyridine complexes, the levels of cytotoxicity are always low, and the only case in which essentially quantitative cell death has occurred is the chloride complex mentioned above. Given the number of examples now reported of such complexes applied in imaging experiments which show low levels of cyctotoxicity and photobleaching, and the similarity observed here with the quantitative cell death seem with the labile halide species, it is likely that the toxicity and photobleaching detected with **Re(1-3)** may be a function of lability, and especially photolability of the pyridine ligands **L(1-3)** in the biological environment.

In contrast, the *meta*-substituted analogues showed the same good levels of uptake, with similar patterns of localisation as those cells which had survived the treatment with the *para* analogues, but in these cases the cell samples remained healthy with no clustering and no significant photobleaching and phototoxicity. The patterns of uptake show a trend which can be explained in terms of lipophilicity, as would be expected for a passive uptake mechanism, with the most highly substituted phenyl alanine analogue **Re-6**, see Figure 8 (D), showing the most intense luminescence, and the alanine and valine derivatives showing similar lower levels of intensity, see Figure 8 (A and B respectively). The patterns of localisation are reminiscent of the now well established patterns observed with monocationic, lipophilic rhenium complexes. In these cases, a general cytoplasmic staining along with more intense mitochondrial and occasional nucleolar localization was observed.

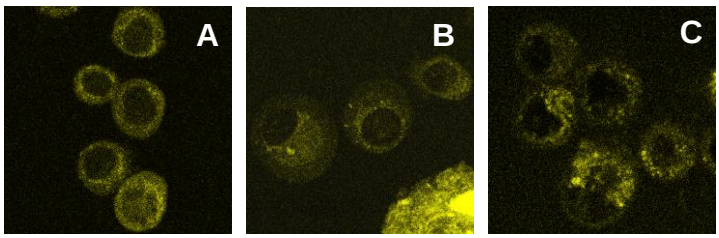

Figure 8. Cell imaging with complex **Re-4, Re-5** and **Re-6** showing localisation (picture A, B and C respectively).

Given this dramatic difference between the cellular behaviour of two apparently closely related sets of complexes a series of experiments were undertaken to probe the mechanism behind their behaviours. NMR studies showed that while ligand displacement occurred in both series of complexes under unnatural conditions ($CDCl_3$, CH_3CN, with competing pyridine ligands), under conditions which matched those of the incubation experiments (DMSO / D_2O with or without competing ligands) no loss of the axial pyridine was observed in either the *para* or *meta* series under physiological conditions, and indeed to observe any ligand exchange at all, high temperature was required. These different rates of ligand exchange in solvents of different polarity can be attributed to differing degrees of solvation of the incoming ligands. It has previously been observed that chloride can displace coordinated pyridines from rhenium *fac* tricarbonyl complexes,[4b] in organic solvents, however this does not occur in aqueous media. Also, it has been shown that an associative mechanism is likely to be at play in these cases,[19] so the nucleophilicity of the incoming ligand is crucial to the rate of displacement. Therefore aqueous media which will allow hydrogen bond donation to the pyridine nitrogen (or other donor atoms) greatly retard the rate of ligand exchange. Thus it appears unlikely that the exchange of ligands in the *para* series occurs during the incubation, and indeed the similar levels of uptake argue against this possibility as had an aqua complex (the product of loss of pyridine in any water-containing medium) been formed, this more polar species would have not shown similar uptake to the *meta* series. Therefore, it seems reasonable that the assumed lability of the *para* series, which is correlated with the observed destruction of cells, is induced in the cells by an as yet unknown mechanism. The photobleaching observed with the *para* series is again unusual, and by analogy with the halide example could indicate photolability of the

axial pyridine, and thus toxicity. However, it is unlikely that phototoxicity alone can explain the unusual images observed with the *para* series, unless the phototoxicity is extremely rapid, as the first images collected showed deformed cells.

A rationalisation of these phenomena could be achieved by consideration of the ease of amino acid radical formation, *i.e.* metal-to-ligand charge transfer excited states of metal complexes can be used to initiate amino acid redox processes. The rate for radical generation can be accelerated by increasing the oxidizing strength of quenched product and also by facilitating the processes for which electrons moves along the species, *i.e.* electron transfer (ET) and photo-induced electron transfer. [20] In that line, and based on studies reported by Nocera *et al.* where is demonstrated that tyrosine oxidation using MLCT excited states of rhenium polypyridyl complexes takes place more easily when intramolecular electron shuttling occurs *via* a unidirectional electron cascade,[21] *para* derivatives should increase this effect over *meta* derivatives. In general, *para*-derivatives allow an easier electronic communication between the metal centre and the *para* substituent, and thus, formation of amino acid radicals would be prompted in those species, Scheme 3. The radical fragment could possibly interact with any endogenous donor and the displacement of the axial pyridine would take place easily. These hypotheses are in concordance with the fact that *para* derivatives suffer photobleaching *in vivo* as well as provoke cellular death in all cases, and none of these effects are observed for their *meta* analogous. Furthermore, it was tested that there is no evidence from prolonged irradiation in a spectrometer of the photo-destruction of the *para* series. Such observation would suggest that a mechanism which involves, rather than intramolecular photolabilisation of the axial pyridine, an intermolecular photo-induced reaction between the excited state of the complexes and an as yet unidentified biological species would also be feasible. This could involve phototoxicity induced by simple radical generation via electron transfer from an endogenous residue, for instance a tyrosine, to the complex. While the exact mechanism of the toxicity of the *para* series is both unclear, and apparently involves reaction with complex biological molecules as it could not be reproduced *in vitro*, the dramatic difference in behaviour between the *para* and *meta* series

demonstrates, again, that apparently small changes in the structures of rhenium complexes can induce profound changes in cellular behaviour.

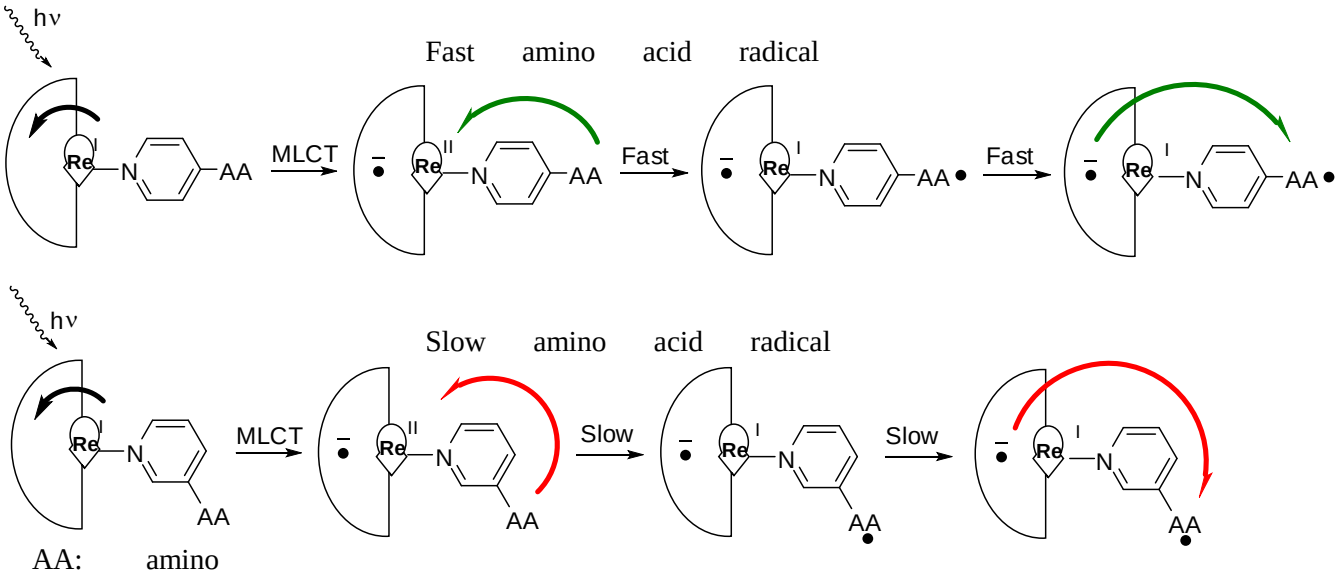

Scheme 3. Depiction of intramolecular electron shuttling for *para*- and *meta*- rhenium analogues respectively.

Conclusions

In summary, we have reported the synthesis of a series of *para*- and *meta*-pyridylamino acid derivatives and their coordination to *fac*-[Re(bipy)$(CO)_3$] units. Photophysical studies of the novel rhenium species showed the typical values for these type of cationic derivatives, *i.e.* emission intensity maxima between 537 and 541 nm, large Stokes shifts (>140 nm) and long lifetimes (270-370 ns). Cell imaging experiments were undertaken using the MCF-7 cell line and *para* and *meta*-rhenium derivatives, which showed a good uptake in both cases but a markedly different effect on the cells. *Para* substituted analogues **Re(1-3)** induced damage in the cell structure, and cells death was observed in all cases. The typical localization pattern of monocationic Re complexes, *i.e* cytoplasmic staining and more intense mitochondrial localization, was observed for a small percentage of healthy cells before undergoing photobleaching. On the contrary, cells incubated with *meta* substituted analogues **Re(4-6)** remained healthy with no clustering and no significant photobleaching and phototoxicity and showed the typical localization pattern for monocationic Re complexes. The different behaviour *in vivo* for both sets of rhenium complexes can be rationalized by the ease of amino acid radical formation in the case of *para* rhenium derivatives in comparison with their *meta*-rhenium analogues. Upon irradiation of the imaging agent, a rapid process of intramolecular and unidirectional shuttling of electrons could be crucial to induce the formation of amino acid radicals in the case of *para* rhenium derivatives. Formation of radicals within the cell imaging agent would prone their interaction with endogenous donors. Exchange processes involving the axial pyridine might occur at this point and thus, translate into the higher toxicity and photobleaching associated with those species. Alternatively, an intermolecular photo-induced reaction between the excited state of the complexes and an as yet unidentified biological species could not be discarded either. Nevertheless, it is evident that small structural changes in rhenium complexes can induce profound variation in cellular behaviour.

Acknowledgements. Authors thank the Ministerio de Economía y Competitividad (MEC/FEDER CTQ2010-20500-C02-01) for financial support. We also thank Prof. David Lloyd and Dr. Anthony J.

Hayes for their comments and help with the cell imaging experiments performed in the Confocal Microscopy Unit at Cardiff School of Biosciences.

Supporting Information. X-ray crystallographic data for **L2** and **R-2** in CIF format. This material is available free of charge via the Internet at http://pubs.acs.org.

---

[1] a) Fernández-Moreira, V.; Thorp-Greenwood, F. L.; Coogan, M. P. *Chem. Commun.* **2010**, *46*, 186. b) Zhao, Q.; Huang, C.; Li, F. *Chem. Soc. Rev.* **2011**, *40*, 2508. c) Balasingham, R. G.; Coogan, M. P.; Thorp-Greenwood, F. L. *Dalton Trans.* **2011**, *40*, 11663. d) Lo, K. K.-W.; Chio, A. W.-T.; Law, W. H.-T. *Dalton Trans.* **2012**, *41*, 6021.

[2] a) Worl, L. A.;. Duesing, R.; Chen, P.; Della Ciana, L.; Meyer, T. J. *J. Chem. Soc., Dalton Trans.* **1991**, 849. b) Stufkens, D. J.; Vlček, Jr. A. *Coord. Chem. Rev.* **1998**, *177*, 127. c) Sacksteder, L. A.; Lee, M.; Demas, J. N.; DeGraff, B. A. *J. Am. Chem. Soc.* **1993,** *115*, 8230.

[3] Lakowicz, J. R.; *Principles of Fluorescence Spectroscopy*, Springer, New York 3rd edn, **2006**. (For a comprehensive and authoritative review of issues related to fluorescence).

[4] a) Fernández-Moreira, V.; Thorp-Greenwood, F. L.; Amoroso, A. J.; Cable, J.; Court, J. B.; Gray, V.; Hayes, A. J.; Jenkins, R. L.; Kiriuki, B. M.; Lloyd, D.; Millet, C. O.; Williams, C. F.; Coogan, M. P. *Org. Biomol. Chem.* **2010**, *8*, 3888. b) Amoroso, A. J.; Arthur, R. J.; Coogan, M. P.; Court, J. B.; Fernández-Moreira, V.; Hayes, A. J.; Lloyd, D.; Millet, C. O.; Pope, J. A. *New J. Chem.* **2008**, *32*, 1097.

[5] a) Lo, K. K.-W.; Zhang, K. Y.; Chung C.-K.; Kwok, K. Y. *Chem.–Eur. J.* **2007**, *13*, 7110. b) Puckett, C. A.; Barton, J. K. *J. Am. Chem. Soc.* **2009**, *131*, 8738. c) Puckett, C. A.; Barton, J. K. *Bioorg Med. Chem.* **2010**, *18*, 3564.

[6] a) Lo, K. K.-W.; Hui, W.-K.; Ng, D. C.-M. *J. Am. Chem. Soc.* **2002**, *124*, 9344. b) Lo, K. K.-W.; Lee, T. K.-M. *Inorg. Chem.* **2004**, *43*, 5275. c) Lo, K. K.-W.; Lau, J. S.-Y. *Inorg. Chem.* **2007**, *46*, 700.

[7] a) Stephenson, K. A.; Banerjee, S. R.; Besenger, T.; Sogbein, O. O.; Levadala, M. K.; McFarlane, N.; Lemon, J. A.; Boreham, D. R.; Maresca, K. P.; Brennan, J. D.; Babich, J. W.; Zubieta, J.; Valliant, J. F. *J. Am. Chem. Soc.* **2004**, *126*, 8598. b) Ferri, E.; Donghi, D.; Panigati, M.; Precipe, G.; D'Alfonso, L.; Zanoni, I.; Baldoli, C.; Maiorana, S.; D'Alfonso, G.; Lincandro, E. *Chem. Commun*. **2010**, *46*, 6255. c) Raszeja, L.; Maghnouj, A.; Hahn, S.; Metzler-Nolte, N. *ChemBioChem.* **2011**, *12*, 371.

[8] a) Viola-Villegas, N.; Rabideau, A. E.; Cesnavicious, J.; Zubieta, J.; Doyle, R. P.; *ChemMedChem* **2008**, *3*, 1387. b) Vortherms, A. R.; Kahkoska, A. R.;. Rabideau, A. E.; Zubieta, J.; Andersen, L. L.; Madsen, M.; Doyle, R. P. *Chem. Commun*. **2011**, *47*, 9792.

[9] Lo, K. K.-W.; Louie, M.-W.; Sze, K.-S.; Lau, J. S.-Y. *Inorg. Chem.* **2008**, *47*, 602.

[10] Josefsen, L. B.; Boyle, R. W. *Met.-Based Drugs* **2008,** *24*, 276109, b) Stochel, G.; Wanat, A.; Kulís, E.; Stasicka, Z. *Coord. Chem. Rev.* **1998**, *171*, 203.

[11] Sheldrick, G. M. *Acta Cryst.* **2008,** *A64,* 112.

[12] Wang, Y.; Lucia, L. A.; Schanze, K. S. *J. Phys.* Chem. **1995**, *99*, 1961.

[13] Blanco-Rodríguez, A. M.; Towrie, M.; Súkora, J.; Zálĭs, S.; Vlček., Jr. A. *Inorg. Chem.* **2011**, *50*, 6122.

[14] Dattelbaum, D. M.; Omberg, K. M.; Schoonover, J. R.; Martin, R. L.; Meyer, T. J. *Inorg. Chem.* **2002**, *41*, 6071.

[15] Uppal, B. S.; Booth, R. K.; Ali, N.; Lockwood, C.; Rice, C. R.; Elliott, P. I. P. *Dalton Trans.* **2011**, *40*, 7610.

[16] a) Kuimova, M.K.; Alsindi, W. Z.; Blake, A. J.; Davies, E. S.; Lampus, D. J.; Matousek, P.; McMaster, J.; Parker, A. W.; Towrie, M.; Sun, X.-Z.; Wilson, C.; George, M. W. *Inorg. Chem.* **2008**,

47, 9857. b) Sacksteder, L.A.; Lee, M.;. Demas, J. N; DeGraff, B. A. *J. Am. Chem. Soc.* **1993**, *115*, 8230.

[17] a) Wu, S.-H.; Abruña, H. D.; Zhong, Y.-W. *Organometallics* **2012**, *31*, 1161. b) Gómez, E.; Huertos, M. A.; Pérez, J.; Riera, L.; Menéndez-Velazquez, A. *Inorg. Chem.* **2010**, *49*, 9527. c). Partyka, D. V.; Deligonul, N.; Washington, M. P.; Gray, T. G. *Organometallics* **2009**, *28*, 5837.

[18] Amoroso, A. J.; Coogan, M. P.; Dunne, J. E.; Fernández-Moreira, V.; Hess, J. B.; Hayes, A. J.; Lloyd, D.; Millet, C. O.; Pope, J. A.; Williams, C. *Chem Commun.* **2007**, 3066.

[19] Fernández-Moreira, V.; Thorp-Greenwood, F. L.; Arthur, R. J.; Kiauri, B. M.; Jenkins, R. L.; Coogan, M. P. *Dalton Trans.* **2010**, *39*, 7493.

[20] A) Reece, S. Y.; Seyedsayamdost, M. R.; Stubbe, J. A.; Nocera, D. G. *J. Am. Chem. Soc.* **2006**, *128*, 13654. b) Ishikita, H.; Soudackov, A. V.; Hammes-Schiffer, S. *J. Am. Chem. Soc.*, **2007**, *129*, 11146.

[21] Reece, S. Y.; Nocera, D. G. *J. Am. Chem. Soc.* **2005**, *127*, 9448.